Journal of Raman Spectroscopy

WILEY

Journal of RAMAN SPECTROSCOPY

RESEARCH ARTICLE

Covert and Multiplexed SERS QR Codes via Inkjet Printing

Zishen Yang | Erin Schnetzer | Mary Tran | Chaoyang Jiang

Department of Chemistry, University of South Dakota, Vermillion, South Dakota, USA

Correspondence: Zishen Yang (Zishen.Yang@usd.edu) | Chaoyang Jiang (CY.Jiang@usd.edu)

Received: 19 December 2024 | **Revised:** 7 September 2025 | **Accepted:** 24 September 2025

Funding: This work was supported by the South Dakota Governor's Office of Economic Development through the Governor's Research Center for Understanding and Disrupting the Illicit Economy, and the National Science Foundation, EEC-2330175.

ABSTRACT

Covert patterns have an extra layer of security protection for anti-counterfeiting labels as compared with the traditional overt ones. To increase the complexity and security of quick response (QR) codes, it would be valuable to make covert QR codes that will be only scannable after a certain decoding process. In this work, the use of surface-enhanced Raman spectroscopy (SERS) is explored to fabricate covert QR codes. Through developing new Raman-active security inks, we can prepare covert QR codes using a convenient inkjet printing method. These QR codes will not be revealed directly. They can only be decoded using a confocal Raman microscope. In addition, multiplex QR codes can be accomplished using multiple Raman probes in printing. Our results showed that the printed QR codes are covert, have strong SERS signals, and can be easily recognized after the SERS decoding. It is anticipated that there is great potential for using such covert and multiplexed SERS-based QR codes for advanced anti-counterfeiting applications.

1 | Introduction

Counterfeiting is a widespread and growing concern, with nearly two-thirds of companies reporting increased activity since the pandemic, according to the International Trademark Association (INTA) [1]. However, many companies are constrained by resources and technology that they can use to fight back efficiently. Due to this demand, various advanced anti-counterfeiting technologies have been explored recently [2–5]. Security labels, widely used in practice, have played an essential role in combating counterfeit goods [6]. Many methods, such as watermarks, barcodes [7–10], and quick response (QR) codes [11–15], have been applied to these security labels. Some of these methods are so popular with the public that they eventually become more prone to counterfeiting. Therefore, it is necessary to design novel technologies with unique security strategies to fabricate multiplexed anti-counterfeiting labels.

One approach to bolster security labels involves using camouflage techniques. Covert labels, which provide extra layers of protection, are much more difficult to reverse engineer than traditional overt labels. Over the past decade, invisible inks, such as UV-active and IR-active dyes, have been developed for security applications [16–18]. Covert patterns or images with concealed information could be hard to notice and thus possess a higher level of security. Recently, Lee et al. prepared a color-coded IR-based anti-counterfeit label using a hybrid planar-plasmonic cavity [19]. The labels can seamlessly blend into the background, and encoded information can only be revealed with the scrutiny of a thermal imaging camera. Overall, it is essential to continually develop innovative functional materials for fabricating covert anti-counterfeiting labels.

Plasmonic materials are of increasing interest in the development of new anti-counterfeiting labels. Several approaches, such as photoluminescence [5, 20–22], radio frequency identification [23, 24], magnetic response [10, 25], and plasmonic interactions [10, 26–29], have been incorporated into advanced security labels. Among these, surface-enhanced Raman scattering (SERS) offers unique advantages, including morphology-dependent enhancement, a wide range of probe molecules, high information density, and relatively low

public familiarity, which improves security [9, 28–35]. Recent studies have explored SERS-based anti-counterfeiting labels, including approaches using printable polymer nanoparticles for invisible information encryption and robust tag recovery, highlighting the growing versatility of printable Raman-active materials [36]. However, current challenges include achieving stable and efficient SERS inks and simplifying fabrication and decoding processes. Recent advances using particle-free silver inks have enabled scalable, inkjet-based fabrication of SERS substrates [28, 37, 38]. Still, few reports have addressed the fabrication of covert, multiplexed SERS QR codes using low-cost, commercially available printers.

In this work, we demonstrate the inkjet printing of covert, multiplexed SERS QR codes using a low-cost, commercially available printer. Silver ink and probe molecules are loaded into separate CMYK chambers for simultaneous deposition. The printed patterns were thermally treated and analyzed by confocal Raman microscopy. Our results show that the QR codes are invisible, SERS-active, and reliably decodable, with flexible probe selection and reusability. This approach offers a practical pathway for scalable, high-security labeling in anti-counterfeiting applications. Unlike some previous SERS patterning strategies that require multiple printing processes, our method enables covert and multiplexed QR code fabrication in a single inkjet printing step. This simplicity enhances reproducibility and supports scalable deployment using standard printing infrastructure.

2 | Experimental Section

2.1 | Chemicals and Materials

Silver nitrate (99%+, ACS reagent) was purchased from Thermo Scientific. Ammonia hydroxide (Certified ACS Plus) was purchased from Fisher Scientific. Formic acid was purchased from MP Biomedicals. 4-Cyanobenzoic acid (4-CBA) was purchased from Oakwood Chemicals. All chemicals and materials were used without further purification.

2.2 | Synthesis of Silver Ink

Silver ink was synthesized using a modified method reported previously [39]. Briefly, silver nitrate (2.00 g) was dissolved in ammonia hydroxide (3.75 mL) while stirring at 700 rpm. Formic acid (0.4 mL) was added to the solution dropwise, and the mixture was further stirred for 5 min. Upon completion, the solution was centrifuged at 10,000 rpm for 10 min and filtered with a 0.45-μm syringe filter. The silver solution was then loaded into an inkjet printer cartridge for printing.

2.3 | Printing of SERS QR codes

The silver ink was loaded into one chamber of the Canon CL-244 ink cartridge and printed with a Canon MG2500 printer. The probe solution, 10 mM 4-CBA, was also loaded into the ink cartridge. Typically, the Raman probe molecules are loaded into other chambers if needed. The printing substrate was HP Premium Photo Paper Plus (Q6568A). The printed substrate was heated in an oven (Isotemp vacuum oven 280A) at 70°C for 30 s after the printing to ensure the complete drying of the ink droplets.

2.4 | Characterization

The printed patterns were examined using a field-emission scanning electron microscope (FE-SEM) (Zeiss). Then, spectral analysis and mapping of the printed patterns were performed using a confocal Raman microscope with an automatic XY stage (Horiba XploRA PLUS). 785 nm laser with a laser intensity of 10% and the 10× objective was used in all the Raman experiments. The exposure time for Raman spectrum acquisition was 1 s, while the mapping exposure time was 0.2 s. The QR codes were modified and pixelated with Piskel.

3 | Results and Discussion

Scheme 1 presents an overall procedure for fabricating the covert QR codes via Inkjet printing. The initial step involves the synthesis of silver ink from $AgNO_3$ as the starting material, which is gradually mixed with formic acid. This method is slightly different compared with the literature, which used silver acetate. In our work, silver nitrate was selected for its high aqueous solubility and strong coordination with ammonia, resulting in Ag $(NH_3)_2^+$ complexes. These complexes are more reactive under mild basic reduction conditions, enabling efficient silver formation without the need for heating. While the fundamental reduction mechanism remains similar (formic acid reduces Ag^+ to Ag^0), the kinetics and intermediate species are expected to differ due to the presence of counterions. Subsequently, the silver ink is loaded with probe molecules into separate chambers of an inkjet cartridge. The generation and color-coding of QR codes ensure precise printing. The printed QR codes are subjected to heat treatment, resulting in a thermal reduction of silver complexes. With that, covert codes not accessible to a direct optical scan can be obtained. However, applying a confocal Raman microscope can decode the QR codes and generate a scannable Raman mapping that contains concealed information within the QR codes.

Achieving accurate Raman mapping in SERS applications depends on high-quality label fabrication. In the case of inkjet printing, poor print quality can distort pixel representation during mapping, compromising the reliability of the decoding process. To investigate the printing quality, we printed basic 25 × 25 arrays on photo paper and studied them using various heat treatments for 30 s, as shown in Figure 1a. While all samples showed a 25 × 25 array pattern, the color of each sample differed significantly with the change in temperature during the heat treatment. The sample with 45°C treatment has a dark yellow hue with indistinct edges and corners, some of which appeared "spiky." On the contrary, the 70°C sample had a dark brown color with clear edges and corners for each block. When viewed from a side angle, a metallic sheen can be observed. At 110°C, the sample became black but suffered from layer separation due to heat compromising the photo paper's layered structure. In addition, UV irradiation was also used to promote

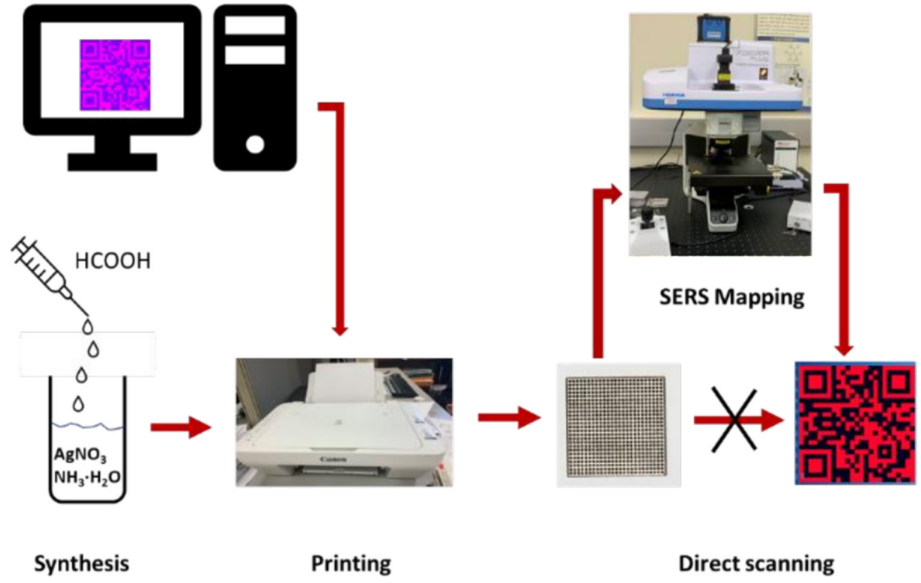

SCHEME 1 | The fabrication process of inkjet printable covert SERS QR codes.

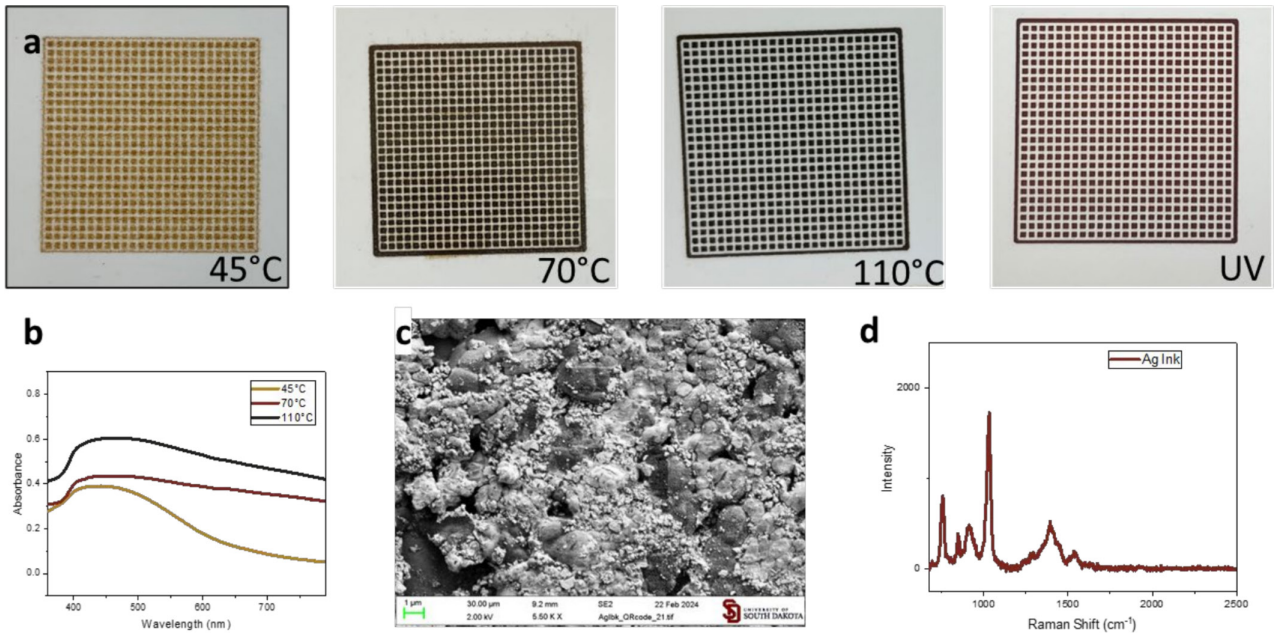

FIGURE 1 | (a) Inkjet print patterns treated under different conditions; (b) absorption spectra of heat-treated samples from the total reflectance data; (c) SEM image of printed Ag patterns on an aluminum foil; (d) Raman spectra printed patterns with the silver ink.

the silver ink reduction after printing. This process was much slower than heating, resulting in a final sample with a dark red hue, and no metallic shine was seen. The absorbance spectra of the heat samples were determined by analyzing the total reflectance measurements (Figure 1 b). A broad absorption can be found for all these samples in a 400- to 600-nm region, with a maximum of about 450 nm. Such an absorption band is typical for silver nanoparticles and can be associated with surface plasmon resonance (SPR). This agrees with our expectation of generating nanosized silver particles with the heat treatment of the printed arrays. We also found a direct correlation between the increased heating temperature and the higher absorption, suggesting a darker coloration of the samples.

To further optimize post-print heat treatment, we conducted a temperature gradient study from 60°C to 100°C in 10°C increments, and the results are presented in the Supporting Information (Figure S1). A modest increase in Raman intensity was observed at temperatures ≥80°C, likely due to enhanced nanoparticle growth. However, these gains were outweighed by significant substrate deformation, including warping and curling of the photo paper, which interfered with Raman mapping due to loss of surface flatness and focus uniformity. In contrast, 70°C produced a strong and stable SERS signal while maintaining excellent substrate integrity, making it the most practical and reproducible treatment condition for covert QR code

fabrication. This balance is critical to ensuring decoding fidelity and real-world applicability.

We used field-emission scanning electron microscopy (FE-SEM) further to elucidate the morphology of the printed silver patterns, as illustrated in Figure 1c. Numerous "rock-like" particles are dispersed across a sizable silver patch. The particle sizes range from a few nanometers to 500 nm. Notably, the silver ink was initially particles-free before printing and drying, indicating that the silver nanoparticles and patches formed during the heating and drying. Our results indicate that printing conditions are essential for producing high-quality prints with well-defined edges and uniform patterns, which could be crucial for achieving accurate Raman mapping in SERS-based applications.

Figure 1d shows the Raman spectrum of the Ag ink alone, without any added probe molecules. It is worth noting that a Raman peak at 1030 cm^{-1} was consistently observed from the printed Ag ink, even in the absence of added probes. This peak is attributed to residual organic species originating from the ink formulation, likely including surface-bound formate or Ag–ammonia complexes formed during the reduction of silver nitrate by formic acid under basic conditions. Similar features have been observed in SERS studies involving carboxylates or C–H deformation vibrations on silver surfaces [40]. Based on the spectrum analysis, we can conclude that the Raman peaks appear well-distributed and easily distinguishable from one another. Two Raman probes were carefully selected in this work to print covert QR codes based on their spectral specificity, chemical stability, and compatibility with inkjet printing. The first probe, 4-cyanobenzoic acid (4-CBA), exhibits a sharp and isolated Raman band at 2232 cm^{-1}, corresponding to its cyano (C≡N) functional group (Figure S2). This peak lies in a typically silent region of the Raman spectrum—well outside the crowded 1200–1500 cm^{-1} range—making it ideal for background-free detection and multiplexed encoding. The second probe, cyan ink from commercial inkjet cartridges, contains dye molecules with strong and reproducible peaks at 1336 and 1539 cm^{-1}, which are well-separated from the 4-CBA signal. Both probes demonstrated high signal consistency after thermal treatment, remained stable in the silver ink matrix, and were compatible with CMYK cartridge loading for scalable printing. These features, combined with their distinct spectral fingerprints, make them well-suited for covert SERS labeling.

The Raman performances of the printed samples under different temperature treatments were examined to understand the impact of post-print thermal treatments. The results (Figure S3) indicated that the samples with either 45°C heating or UV treatments had minimal to no Raman signal, while the ones with 70°C and 110°C exhibited comparable Raman intensity. This result agrees well with the absorption spectra discussed above. The lack of SERS signals for the 45°C treated sample can be due to the very low (if any) absorption at 780 nm. On the other hand, the samples treated with 70 or 110°C have some absorption at 780 nm, thus resulting in strong SERS signals, likely related to the collective SPRs of the silver nanoparticles. Consequently, 70°C was an ideal heat treatment temperature for subsequent experiments. Notably, samples with a metallic sheen also demonstrated high Raman intensity, a valuable insight into predicting Raman performance during fabrication.

The feasibility of employing printed SERS QR codes for anti-counterfeiting was further explored. A straightforward, overt QR code was produced and assessed as a first step. We converted a QR code into binary colors of magenta and white (Figure 2a) as

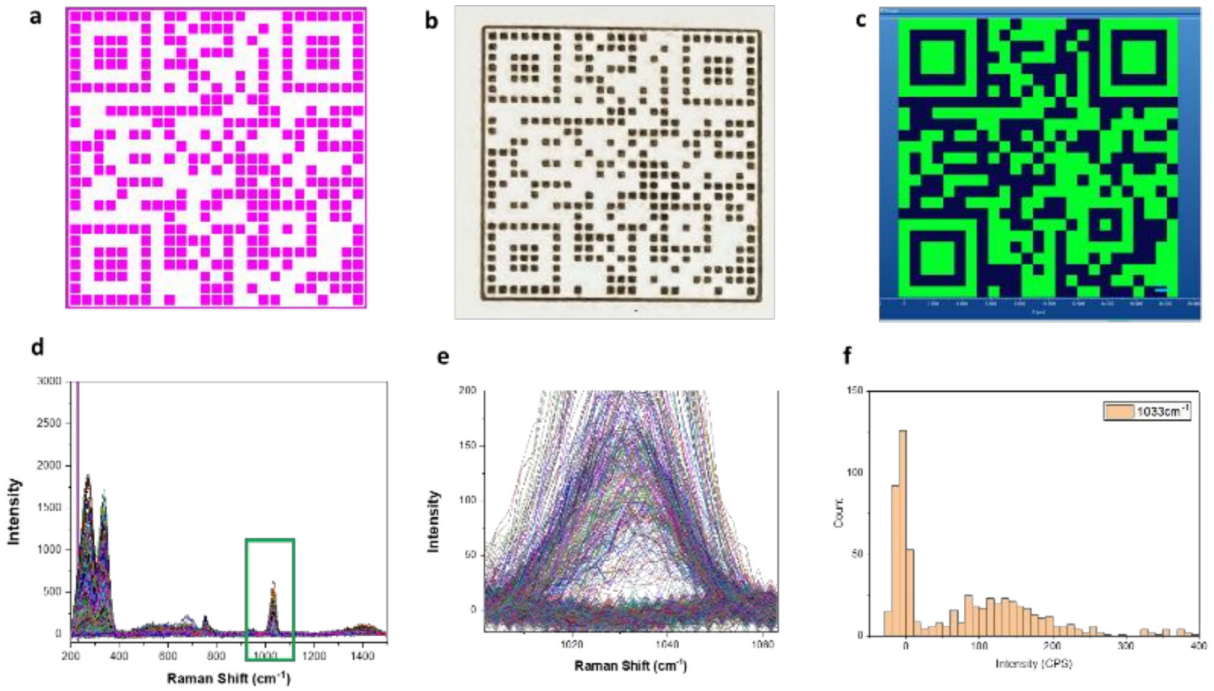

FIGURE 2 | (a) Pixelated QR code designed for printing. (b) Overt QR code after the heat treatment. (c) Generated QR code with SERS mapping. (d) SERS spectra of the printed patterns at all the pixels. (e) enlarged spectrum of peak 1030 cm^{-1}. (f) Intensity distribution of the SERS peak at 1030 cm^{-1}.

our silver ink was filled in the magenta chamber of the cartridge. When printed, the desired silver ink will cover the magenta area, while the white blocks are uncovered. The printed QR code appeared dark brown upon heat treatment. This QR code is unscannable at a close distance due to the gridlines breaking up the QR code pattern but scannable at a further distance (Figure 2b). We have successfully printed these QR codes in various sizes. Due to the limited printing resolution of the cheap commercial printer, we can readily print scannable QR codes with a minimum size of 10 mm in length (Figure S6).

Raman mapping was employed on the samples to transform this pattern into a QR code that can be easily scanned (Figure 2c). The peak intensity at 1030 cm^{-1} was chosen for the Raman mapping, as depicted in Figure 2d. When enlarging the green box region, a clear intensity gap is visible, which indicates the peak intensities could be separated into two groups (Figure 2e): Raman signals and spectral background (noise). All the 1030 cm^{-1} peak intensities from the mapping process were constructed into a histogram, and a cutoff of 22 was selected by the data analysis, which will be used to reconstruct the QR code. All the pixels with an intensity lower than 22 will be designated as black, while those greater than that will be colored (green was used here). The resulting SERS mapping successfully replicated the initial design and was fully scannable, as evidenced in Figure 2c. This approach, which involves pixel design, fabrication, and Raman mapping, would be a recommended protocol for creating more elaborate multiplexed QR codes.

A covert QR code, in which the QR pattern cannot be scanned in a simple, direct manner, will be produced by managing the pixelated pattern of a QR code during the inkjet printing process. For example, 4-CBA probe molecules can be loaded into a cartridge's "yellow" chamber, while the silver ink is in the "magenta" chamber. We can easily tell the computer to print QR codes with pixels containing pure silver ink or a mixture of silver ink and 4-CBA probe molecules. Figure 3a shows a design of the dual color (red/pink) QR codes that we input into a computer. With careful optimization, we can make these two types of pixels have very similar visual appearances after printing. As shown in the photo of the print label, it turns out that the printed pattern is more like a simple 25 × 25 array than a QR code. Because all these pixels in the QR code are very similar, this QR code cannot be scanned directly by any phone or scanner, and no valuable information can be extracted from this image alone.

Such covert QR codes can only be decoded by the process of Raman mapping, including both experimental acquisition and data process. After acquiring a set of Raman spectra at each pixel, we used the Raman peak's intensity at 2232 cm^{-1} for decoding. The resulting SERS mapping, depicted in Figure 3c, again reproduced the originally designed QR code, and the SERS map is highly accurate and fully scannable. It is worth noting that cyan ink can also serve as the Raman probe for this application. With a low concentration of cyan in printed patterns, the QR codes are covert to the naked eye while fully scannable after Raman decoding. In addition, if needed, we can also manipulate

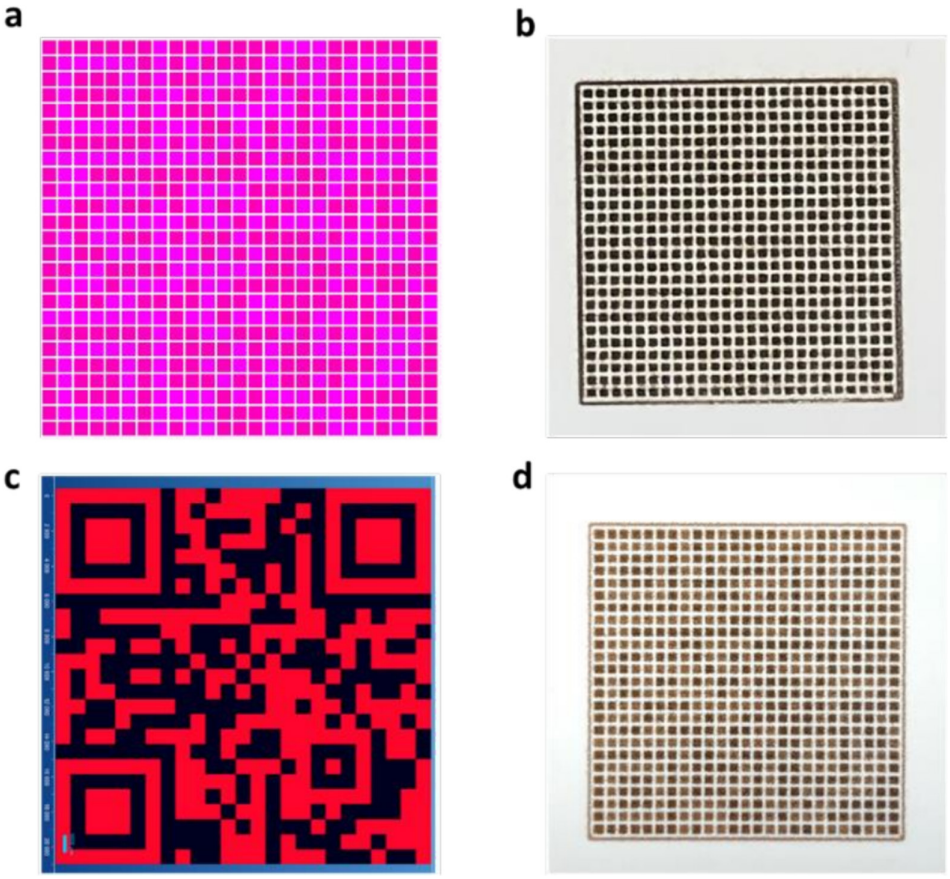

FIGURE 3 | (a) Pixelated QR code design for covert QR code; (b) printed and heat-treated covert QR code; (c) SERS mapping of the covert QR code; (d) slightly visible QR code printed with 50% cyan probe and 50% silver ink.

the appearance of printed QR codes by adjusting the probe-to-ink ratio. For example, the QR code was tuned to be slightly visible when we printed it with a 50% cyan probe and 50% ink, as shown in Figure 3d. Therefore, we can switch between covert and overt appearances during the printing process by exploring and altering probe concentrations and amounts.

To further understand the impact of printed probe density on SERS performance and stealth, we examined the Raman intensity of QR codes printed with 4-CBA (10 mM) at grayscale levels of 25%, 50%, 75%, and 100%. As shown in the Supporting Information (Figure S4), the Raman peak intensity at 2232 cm^{-1} increases with grayscale level, from approximately 90 (25%) to 180 counts (100%). Despite this trend, the 25% condition produced sufficient SERS signal for QR code decoding while maintaining the covert appearance of the printed pattern. These results demonstrate that low grayscale levels offer a practical compromise, enabling both strong SERS detection and high visual covertness for anti-counterfeiting applications.

An even more effective method for enhancing the security of QR codes is to store a hidden QR code behind an apparent one or hide two codes in one, making it extremely difficult for counterfeiters to reverse-engineer. This is accomplished by printing a complex dual covert "QR code" composed of two overlapping QR codes. These QR codes are of equal size and dimension, but will lead to different sets of information. In this work, one QR code uses silver ink with 25% 4-CBA as a probe, while the other incorporates silver ink with 15% cyan ink. Experimentally, the "magenta" chamber contains Ag ink, the "yellow" chamber holds 4-CBA, and the "cyan" chamber carries cyan ink. The QR code utilizing the 4-CBA probe is printed in pink, while the cyan probe QR code is printed in purple, and the overlay sections are printed with a color that is a combination of both pink and purple (Figure 4a,b). As seen in Figure 4c, the resulting printed QR code presents a highly uniform appearance. It looks like a normal QR code. However, that code is impossible to scan because it overlays two QR codes. By using Raman mapping, this complex pattern can be decoded into two distinct QR codes: one utilizing the 1600 cm^{-1} peak from 4-CBA and the other employing the 1539 cm^{-1} peak from cyan (Figure 4d). Ultimately, we can use the Raman map to re-generate and scan these two QR codes to retrieve the storage information fully. Be aware that the QR codes in this example have relatively low error tolerance by their design, allowing minimal room for incorrect pixels (false positives/negatives) while remaining scannable. In practical applications, QR codes usually have larger dimensions and a higher error tolerance, making them suitable for mass production and streamlining printing while maintaining high complexity and security.

To assess the durability of printed silver QR codes under realistic usage conditions, we subjected samples to environmental stress tests, including mechanical brushing, exposure to sunlight, and high-humidity storage over a 4-week period. After treatment, the QR codes retained their covert appearance with no visible scratching or delamination and remained fully decodable via Raman mapping (Figure S5). The SERS signal intensity and peak position showed no significant change, indicating good mechanical and environmental stability. These results support the potential of our printed SERS QR codes for long-term use in practical anti-counterfeiting applications.

Finally, we applied the inkjet printing of covert QR codes in two real-world scenarios. First, we printed the covert QR code on commercially available blank labels (Avery). As shown in

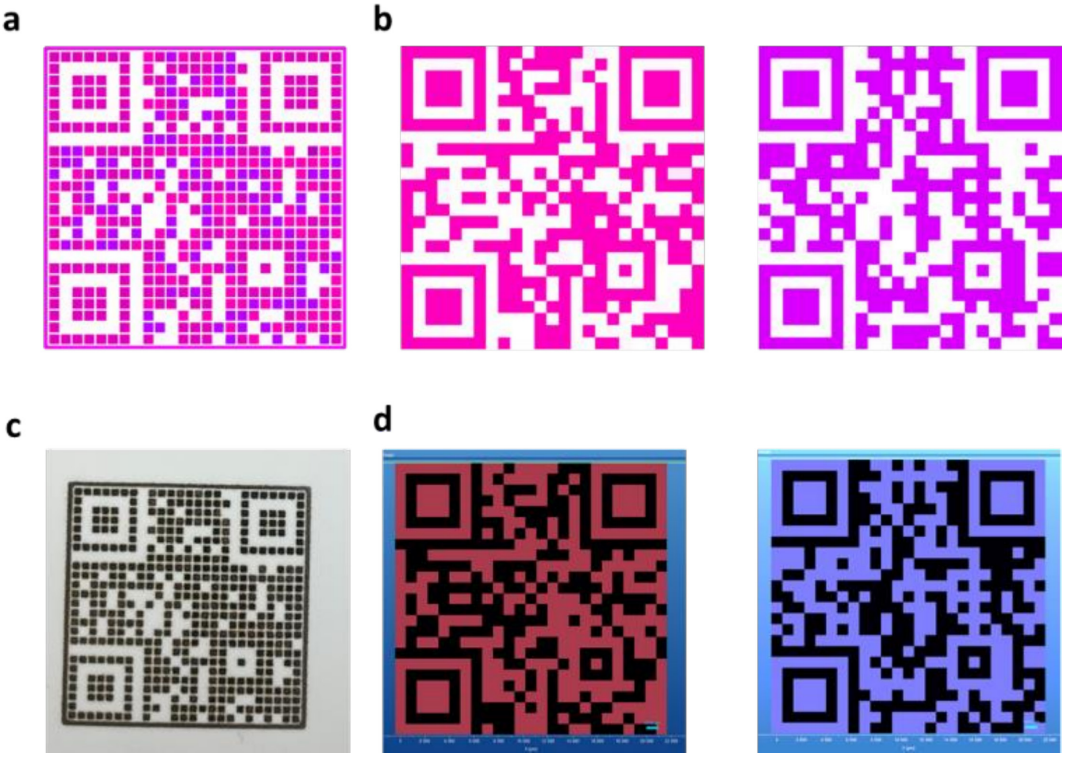

FIGURE 4 | (a) Pixelated dual QR code design; (b) left: QR code with RGB color code (255, 0, 191); right: QR code with RGB color code (217, 0, 255); (c) optical image of the dual QR code; (d) SERS mapping of the two different QR codes.

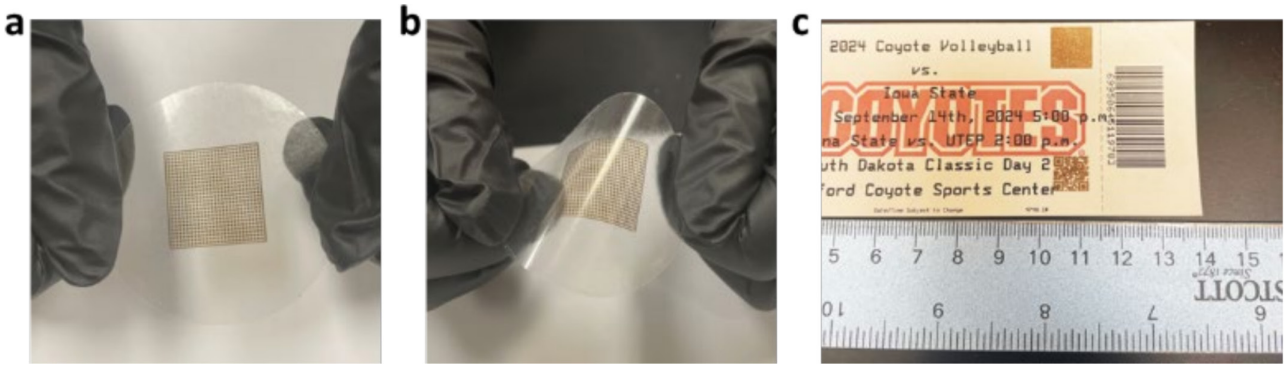

FIGURE 5 | (a) Covert QR code printed on transparent labels; (b) the printed labels show good flexibility by bending; (c) overt and covert QR codes printed on the ticket of a volleyball game.

Figure 5a, the printed QR code has sharp edges and consistent color distribution. This QR code remains covert, with no visible information on the label unless there is a process of Raman decoding. The printed labels also exhibited flexibility (Figure 5b) and could be applied to other surfaces if needed (Figure S7). In addition, we printed our QR codes directly onto a real ticket for the college volleyball game (Figure 5c). Here, the QR codes were smaller than half an inch. The overt QR code was scannable (Figure S8), while the covert one was not, demonstrating that this inkjet printing technique can be applied to various substrates, producing invisible QR codes to the naked eye. This versatility highlights the potential of our inkjet printing of covert QR code technique for a wide range of security and anti-counterfeiting applications. By extending its use to covert barcodes, patterns, or hidden messages, this method could offer an adaptable and cost-effective solution for protecting valuable documents, tickets, or products from unauthorized duplication.

Compared with conventional anti-counterfeiting techniques, such as fluorescent tagging, UV-reactive inks, watermarks, and standard barcodes, our SERS-based QR codes offer several distinct advantages. They are invisible under ambient conditions, unlike fluorescence or watermarks which often require specific lighting or are partially visible to the eye. The use of Raman-active probes enables precise molecular-level encoding, which is inherently difficult to duplicate. In addition, our system allows multiplexed data storage using various probes and is compatible with low-cost, commercially available inkjet printers. The printed labels can also be reconfigured or refreshed for reusability. While optical tags such as holograms and fluorescence may be easier to scan under casual inspection, our covert SERS QR codes are more suitable for applications requiring discreet and high-security verification. This technique can also be used in combination with conventional labels to create robust, multilayered anti-counterfeiting systems.

4 | Conclusion

In conclusion, we have presented the step-by-step process of creating inkjet printable SERS active QR codes. These codes are very versatile as they can be printed overtly or covertly. The covert QR codes are undetectable by traditional methods but can only be scanned after Raman map decoding. We have observed a high correlation between the Raman mapping outcomes and the QR code design, indicating the superior quality of the printing. Additionally, we have explored printing dual complex QR codes to form a composite "pseudo" QR code that can only be decrypted through appropriate Raman mapping. We also demonstrated using this method to fabricate flexible security labels that could be applied to other surfaces. Finally, we printed QR codes directly on normal tickets, presenting the versatility of this method. A key advantage of our strategy is that both the silver ink and multiple Raman probes can be printed simultaneously in a single step using standard CMYK cartridges. This simplifies fabrication compared with multistep or layered approaches reported in other SERS-based labeling systems. Our research findings demonstrate that inkjet printable covert SERS active QR codes are feasible for various applications, highlighting their adaptability, security features, and scalability for widespread use.

Given their covert nature, molecular specificity, and multiplexing capacity, these SERS QR codes hold strong potential for real-world anti-counterfeiting applications. They can be applied to high-value documents, certificates, currency, luxury goods, and artworks, where invisibility and high-density encoding are particularly valuable. Furthermore, this platform could be integrated with existing anti-counterfeiting strategies, such as fluorescent tags, holographic films, or digital verification systems, to create multilayered security protocols. The ability to dynamically reprint and reuse labels with different probes also makes this approach attractive for trackable, renewable security systems. Future work will explore these integration opportunities and evaluate label performance under practical usage conditions.

Acknowledgments

This work is partially funded by the South Dakota Governor's Office of Economic Development through the Governor's Research Center for Understanding and Disrupting the Illicit Economy. This research is based upon work partially supported by the National Science Foundation under award number EEC-2330175 for the Engineering Research Center EARTH.

Conflicts of Interest

The authors declare no conflicts of interest.

Data Availability Statement

The data that support the findings of this study are available from the corresponding author upon reasonable request.

References

1. H. Rother, Anti-Counterfeiting and Online Brand Enforcement: Global Guide, World Trademark Review, (2024).

2. S. Xiong, Y. Xiong, D. Wang, et al., "Achieving Tunable Organic Afterglow and UV-Irradiation-Responsive Ultralong Room-Temperature Phosphorescence From Pyridine-Substituted Triphenylamine Derivatives," *Advanced Materials* 35, no. 28 (2023): 2301874, https://doi.org/10.1002/adma.202301874.

3. M. Li, G. Ren, W. Yang, and Q. Pan, "Photo-Functionalized Metal-Organic Frameworks for Anti-Counterfeiting Applications," *CrystEngComm* 25, no. 5 (2023): 704–714, https://doi.org/10.1039/d2ce01519f.

4. G. Y. Cai, T. Delgado, C. Richard, and B. Viana, "ZGSO Spinel Nanoparticles With Dual Emission of NIR Persistent Luminescence for Anti-counterfeiting Applications," *Materials* 16, no. 3 (2023): 1132, https://doi.org/10.3390/ma16031132.

5. T. Zhang, L. Wang, J. Wang, et al., "Multimodal Dynamic and Unclonable Anti-Counterfeiting Using Robust Diamond Microparticles on Heterogeneous Substrate," *Nature Communications* 14, no. 1 (2023): 2507, https://doi.org/10.1038/s41467-023-38178-1.

6. S. D. Johnson, J. M. Blythe, M. Manning, and G. T. W. Wong, "The Impact of IoT Security Labelling on Consumer Product Choice and Willingness to Pay," *PLoS ONE* 15, no. 1 (2020): 0227800, https://doi.org/10.1371/journal.pone.0227800.

7. M. Wang, B. Duong, H. Fenniri, and M. Su, "Nanomaterial-Based Barcodes," *Nanoscale* 7, no. 26 (2015): 11240–11247, https://doi.org/10.1039/c5nr01948f.

8. S. Shikha, T. Salafi, J. T. Cheng, and Y. Zhang, "Versatile Design and Synthesis of Nano-Barcodes," *Chemical Society Reviews* 46, no. 22 (2017): 7054–7093, https://doi.org/10.1039/c7cs00271h.

9. S. Pekdemir, H. H. Ipekci, M. Serhatlioglu, C. Elbuken, and M. S. Onses, "SERS-Active Linear Barcodes by Microfluidic-Assisted Patterning," *Journal of Colloid and Interface Science* 584 (2021): 11–18, https://doi.org/10.1016/j.jcis.2020.09.087.

10. D. Li, L. Tang, J. Wang, X. Liu, and Y. Ying, "Multidimensional SERS Barcodes on Flexible Patterned Plasmonic Metafilm for Anticounterfeiting Applications," *Advanced Optical Materials* 4, no. 10 (2016): 1475–1480, https://doi.org/10.1002/adom.201600247.

11. M. L. You, M. Lin, S. R. Wang, et al., "Three-Dimensional Quick Response Code Based on Inkjet Printing of Upconversion Fluorescent Nanoparticles for Drug Anti-Counterfeiting," *Nanoscale* 8, no. 19 (2016): 10096–10104, https://doi.org/10.1039/c6nr01353h.

12. Y. Yang, Y. Li, Y. Chen, et al., "Dynamic Anticounterfeiting Through Novel Photochromic Spiropyran-Based Switch@Ln-MOF Composites," *ACS Applied Materials & Interfaces* 14, no. 18 (2022): 21330–21339, https://doi.org/10.1021/acsami.2c01113.

13. Y. M. Wang, X. T. Tian, H. Zhang, Z. R. Yang, and X. B. Yin, "Anticounterfeiting Quick Response Code With Emission Color of Invisible Metal-Organic Frameworks as Encoding Information," *ACS Applied Materials & Interfaces* 10, no. 26 (2018): 22445–22452, https://doi.org/10.1021/acsami.8b06901.

14. S. Tian, P. Feng, S. Ding, Y. Wang, and Y. Wang, "A Color-Tunable Persistent Luminescence Material LiTaO3:Pr3+ for Dynamic Anti-Counterfeiting," *Journal of Alloys and Compounds* 899 (2022): 163325, https://doi.org/10.1016/j.jallcom.2021.163325.

15. J. M. Meruga, W. M. Cross, P. S. May, Q. Luu, G. A. Crawford, and J. J. Kellar, "Security Printing of Covert Quick Response Codes Using Upconverting Nanoparticle Inks," *Nanotechnology* 23, no. 39 (2012): 395201, https://doi.org/10.1088/0957-4484/23/39/395201.

16. H. Q. Zhao, X. C. Qin, L. Zhao, et al., "Invisible Inks for Secrecy and Anticounterfeiting: From Single to Double-Encryption by Hydrochromic Molecules," *ACS Applied Materials & Interfaces* 12, no. 7 (2020): 8952–8960, https://doi.org/10.1021/acsami.0c00462.

17. J. Lee, S. G. Kong, T. Y. Kang, B. Kim, and O. Y. Jeon, "Invisible Ink Mark Detection in the Visible Spectrum Using Absorption Difference," *Forensic Science International* 236 (2014): 77–83, https://doi.org/10.1016/j.forsciint.2013.12.024.

18. P. Dinake, G. N. Phokedi, J. Mokgadi, et al., "An Innovative Microwave-Assisted One-Step Green Synthetic Approach of Biowaste Derived Fluorescent Carbon-Dot Invisible Ink for Currency Anti-Counterfeiting Applications," *Nano* 17, no. 4 (2022): 2250029, https://doi.org/10.1142/s1793292022500291.

19. J. H. Lee, Y. J. Kim, Y. J. Yoo, et al., "Colored, Covert Infrared Display Through Hybrid Planar-Plasmonic Cavities," *Advanced Optical Materials* 9, no. 17 (2021): 2100429, https://doi.org/10.1002/adom.202100429.

20. Y. X. Zhuang, Y. Lv, L. Wang, et al., "Trap Depth Engineering of $SrSi_2O_2N_2$:Ln^{2+},Ln^{3+} (Ln^{2+} = Yb, Eu; Ln^{3+} = Dy, Ho, Er) Persistent Luminescence Materials for Information Storage Applications," *ACS Applied Materials & Interfaces* 10, no. 2 (2018): 1854–1864, https://doi.org/10.1021/acsami.7b17271.

21. X. Zhu, T. Wang, Z. Liu, et al., "A Temporal and Space Anti-Counterfeiting Based on the Four-Modal Luminescent Ba(2)Zr(2)Si(3)O(12) Phosphors," *Inorganic Chemistry* 61, no. 7 (2022): 3223–3229, https://doi.org/10.1021/acs.inorgchem.1c03712.

22. Y. S. Zhou, G. Zhao, J. M. Bian, et al., "Multiplexed SERS Barcodes for Anti-Counterfeiting," *ACS Applied Materials & Interfaces* 12, no. 25 (2020): 28532–28538, https://doi.org/10.1021/acsami.0c06272.

23. R. Singh, E. Singh, and H. S. Nalwa, "Inkjet Printed Nanomaterial Based Flexible Radio Frequency Identification (RFID) Tag Sensors for the Internet of Nano Things," *RSC Advances* 7, no. 77 (2017): 48597–48630, https://doi.org/10.1039/c7ra07191d.

24. G. Khalil, R. Doss, and M. Chowdhury, "A Novel RFID-Based Anti-Counterfeiting Scheme for Retail Environments," *IEEE Access* 8 (2020): 47952–47962, https://doi.org/10.1109/access.2020.2979264.

25. B. Song, H. Y. Wang, Y. L. Zhong, B. B. Chu, Y. Y. Su, and Y. He, "Fluorescent and Magnetic Anti-Counterfeiting Realized by Biocompatible Multifunctional Silicon Nanoshuttle-Based Security Ink," *Nanoscale* 10, no. 4 (2018): 1617–1621, https://doi.org/10.1039/c7nr06337g.

26. Y. Zheng, C. Jiang, S. H. Ng, et al., "Unclonable Plasmonic Security Labels Achieved by Shadow-Mask-Lithography-Assisted Self-Assembly," *Advanced Materials* 28, no. 12 (2016): 2330–2336, https://doi.org/10.1002/adma.201505022.

27. N. Sun, Z. Chen, Y. Wang, S. Wang, Y. Xie, and Q. Liu, "Random Fractal-Enabled Physical Unclonable Functions With Dynamic AI Authentication," *Nature Communications* 14, no. 1 (2023): 2185, https://doi.org/10.1038/s41467-023-37588-5.

28. F. Sahin, S. Pekdemir, M. Sakir, Z. Gozutok, and M. S. Onses, "Transferrable SERS Barcodes," *Advanced Materials Interfaces* 9, no. 17 (2022): 2200048, https://doi.org/10.1002/admi.202200048.

29. S. J. Liu, X. R. Tian, J. Q. Guo, et al., "Multi-Functional Plasmonic Fabrics: A Flexible SERS Substrate and Anti-Counterfeiting Security Labels With Tunable Encoding Information," *Applied Surface Science* 567 (2021): 150861, https://doi.org/10.1016/j.apsusc.2021.150861.

30. Y. Sun, D. Lou, W. Liu, Z. Zheng, and X. Chen, "SERS Labels for Optical Anticounterfeiting: Structure, Fabrication, and Performance," *Advanced Optical Materials* 11, no. 6 (2023): 2201549, https://doi.org/10.1002/adom.202201549.

31. Y. F. Huo, Z. S. Yang, T. Wilson, and C. Y. Jiang, "Recent Progress in SERS-Based Anti-Counterfeit Labels," *Advanced Materials Interfaces* 9, no. 17 (2022): 2200201, https://doi.org/10.1002/admi.202200201.

32. Y. F. Huo, S. Curry, A. Trowbridge, X. R. Xu, and C. Y. Jiang, "Surface-Enhanced Raman Scattering-Based Molecular Encoding With Gold Nanostars for Anticounterfeiting Applications," *Materials Advances* 2, no. 15 (2021): 5116–5123, https://doi.org/10.1039/d1ma00348h.

33. L. Liang, H. Sun, Y. Wu, et al., "Surface-Enhanced Raman Scattering-Encoded Gold Nanostars for Multiplexed Steganographic Anticounterfeiting Labels," *ACS Applied Nano Materials* 7, no. 18 (2024): 21791–21799, https://doi.org/10.1021/acsanm.4c03742.

34. D. Yu, W. Zhu, and A.-G. Shen, "Raman Encoding for Security Labels: A Review," *Nanoscale Advances* 5, no. 23 (2023): 6365–6381, https://doi.org/10.1039/D3NA00707C.

35. D. Yu, Y. Shen, W. Zhu, J.-M. Hu, and A.-G. Shen, "Raman Inks Based on Triple-Bond-Containing Polymeric Nanoparticles for Security," *Nanoscale* 14, no. 21 (2022): 7864–7871, https://doi.org/10.1039/D2NR00788F.

36. W. Zhu, Y. Tang, S. Hu, et al., "Three-Dimensional Printable Triple-Bonded Polymer Nanoparticles for Invisible Information Encryption and Robust Anti-Counterfeiting," *ACS Materials Letters* 7, no. 6 (2025): 2343–2351, https://doi.org/10.1021/acsmaterialslett.5c00464.

37. J.-j. Chen, J. Zhang, Y. Wang, Y.-l. Guo, and Z.-s. Feng, "A Particle-Free Silver Precursor Ink Useful for Inkjet Printing to Fabricate Highly Conductive Patterns," *Journal of Materials Chemistry C* 4, no. 44 (2016): 10494–10499, https://doi.org/10.1039/C6TC03719D.

38. E. P. Hoppmann, W. W. Yu, and I. M. White, "Highly Sensitive and Flexible Inkjet Printed SERS Sensors on Paper," *Methods* 63, no. 3 (2013): 219–224, https://doi.org/10.1016/j.ymeth.2013.07.010.

39. S. B. Walker and J. A. Lewis, "Reactive Silver Inks for Patterning High-Conductivity Features at Mild Temperatures," *Journal of the American Chemical Society* 134, no. 3 (2012): 1419–1421, https://doi.org/10.1021/ja209267c.

40. J. Rathod, C. Byram, R. K. Kanaka, et al., "Hybrid Surface-Enhanced Raman Scattering Substrates for the Trace Detection of Ammonium Nitrate, Thiram, and Nile Blue," *ACS Omega* 7, no. 18 (2022): 15969–15981, https://doi.org/10.1021/acsomega.2c01095.

Supporting Information

Additional supporting information can be found online in the Supporting Information section. **Figure S1:** (a) Percent reflectance, (b) calculated absorption, and (c) SERS spectrum of post-print QR codes at various heat treatment temperatures. **Figure S2:** Raman spectra printed patterns with Ag ink, Ag ink with 4-CBA, and Ag ink with cyan ink, respectively. **Figure S3:** Raman spectra of different curing temperatures. **Figure S4:** SERS spectrum of 4-CBA printed at different print intensities. **Figure S5:** Optical image of Covert SERS labels after (a) 30 days storage in sunlight, (b) 30 days storage in 60% humidity room, (c) brushing with a paint brush, and (d) Raman mapping of covert SERS QR label after storage for 30 days in sunlight. **Figure S6:** Various printed-size QR codes. **Figure S7:** Printed covert labels could be applied to the backside of a monitor. **Figure S8:** Scannable direct printed QR code on a ticket.